

Online Jacobian Estimation and Tracking Control of a Two-Section Tendon-Driven Continuum Robot

Ivan Adi Kuncara¹ and Ayoung Hong^{1,*}

Abstract—This paper proposes a control framework for a two-section, concentrically tendon-driven continuum robot. The tracking control is formulated based on a Jacobian approach using zeroing dynamics. The Jacobian is estimated online from input–output data, using applied tendon force as inputs and measured tip positions as outputs, without requiring an explicit model. Tendon force is employed as the control input to better account for the deformation under external loads. The proposed framework is experimentally validated on a real-scale continuum robot, with tip-position feedback from a stereovision system. Experimental results demonstrate that the robot tip follows the desired trajectory with an RMSE of about 1.18 mm, while maintaining good performance under unknown external loads.

I. INTRODUCTION

Tendon-driven notched backbone continuum robots are widely studied for medical use due to their flexibility and a central lumen for tools or camera. [1]. In particular, concentric multi-section continuum robots improve workspace and dexterity by allowing a smaller robot to translate and rotate within a larger one [2]. A multi-section continuum robot can be modeled as a manipulator and controlled using Jacobian-based methods. However, due to its structural complexity, the robot is subject to model uncertainties induced by tendon friction, inter-section interactions, torsional–axial deformation, and strong coupling effects [3]. These factors hinder accurate model-based Jacobian derivation and can degrade the performance of Jacobian-based tracking control.

In this paper, we address this limitation by proposing a Jacobian-based tracking control framework for a two-section concentric tendon-driven continuum robot. The Jacobian is estimated online from input-output data rather than derived from an explicit model and is used for tip tracking control.

Tendon force-based actuation is used because it better handles deformation under external loads than tendon length-based actuation. The proposed framework is validated through experiments on a real-scale continuum robot.

II. CONTINUUM ROBOT SYSTEM

The system of the continuum robot is illustrated in Fig. 1, consisting of a continuum robot, a passive section, and an actuation unit. The continuum robot comprises two concentrically backbone-type sections, each driven by three tendons. The inner section is capable of translating and rotating within the outer section. The overall diameter of the robot is

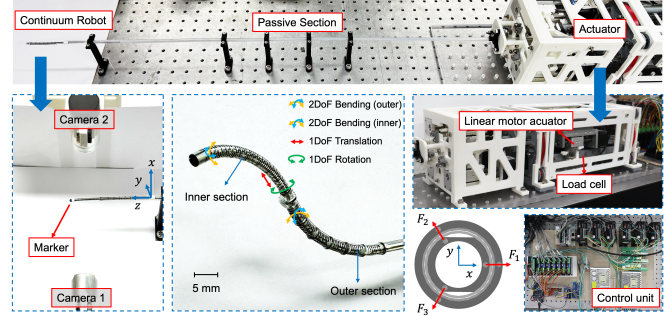


Fig. 1. Overview of the continuum robot system, consisting of two concentric sections and the associated actuation unit.

approximately 4.1 mm, with 1.8 mm of a working channel. The continuum robot is attached to a passive section, which facilitates insertion through natural orifices to reach the target site. All tendons driving both sections pass through the passive section and are connected to load cells for force measurement, which are mounted on linear motor actuators.

To measure the three-dimensional tip position of the continuum robot for feedback control, two Microsoft LifeCam cameras are positioned as shown in Fig. 1. A blue marker is attached to the robot tip, and its position is obtained by calibrating pixel coordinates to real-world distances. Since only the 3D position is available, this study focuses on position control using tendon force inputs, while the translation and rotation of the inner section are not considered.

III. CONTROL FRAMEWORK

The forward kinematic model based on static model of the continuum robot can be expressed as:

$$\mathbf{p}(t) = \mathbf{f}(\mathbf{F}(t)), \quad (1)$$

where $\mathbf{p} = [p_x, p_y, p_z]^T$ denotes the tip position of the continuum robot, and $\mathbf{F} = [F_{o1}, F_{o2}, F_{o3}, F_{i1}, F_{i2}, F_{i3}]^T$ is the tendon forces of the outer (\cdot)_o and inner (\cdot)_i sections. The mapping $\mathbf{f} : \mathbb{R}^6 \rightarrow \mathbb{R}^3$ denotes the nonlinear forward kinematics that relates the tendon forces to the tip position.

Based on (1), to drive the tip position $\mathbf{p}(t)$ toward the desired position $\mathbf{p}_d(t)$, a tracking controller based on a zeroing dynamics approach and the Jacobian matrix is employed:

$$\dot{\mathbf{F}}(t) = \mathbf{J}(t)^\dagger (\dot{\mathbf{p}}_d(t) + k_p(\mathbf{p}_d(t) - \mathbf{p}(t))), \quad (2)$$

where \dagger denotes the pseudoinverse, $\mathbf{p}(t)$ is obtained from the camera system, and k_p is a positive gain. The Jacobian \mathbf{J} is typically obtained by differentiating (1) with respect to time. However, due to the complexity and inaccuracy of

¹Department of Mechanical Engineering, Chonnam National University, Gwangju 61186, Republic of Korea.

*Corresponding email: ahong@jnu.ac.kr.

This work was supported by the National Research Foundation of Korea (NRF) grant funded by the Korea government (MSIT) (RS-2024-00340040).

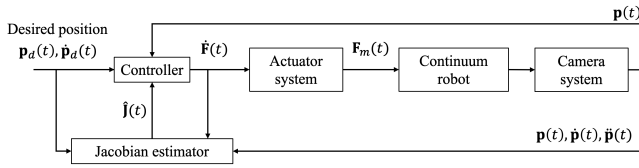


Fig. 2. Proposed control framework for tip tracking based on an estimated Jacobian.

the forward kinematic model, an estimated Jacobian $\hat{\mathbf{J}}(t)$ is adopted and updated online using input–output data without requiring an explicit model.

The estimated Jacobian is updated according to [4]:

$$\dot{\hat{\mathbf{J}}}(t) = \left(\ddot{\mathbf{p}}(t) - \hat{\mathbf{J}}(t)\ddot{\mathbf{F}}(t) + k_J(\dot{\mathbf{p}}(t) - \hat{\mathbf{J}}(t)\dot{\mathbf{F}}(t)) \right) \dot{\mathbf{F}}(t)^\dagger, \quad (3)$$

where k_J is a positive adaptation gain. Since the vision system provides only position measurements, the velocity $\dot{\mathbf{p}}(t)$ and acceleration $\ddot{\mathbf{p}}(t)$ are numerically obtained using Euler-type differentiation ($\dot{\mathbf{p}}(t) \approx (\mathbf{p}(t) - \mathbf{p}(t-1))/dt$); the same applies to $\ddot{\mathbf{F}}(t)$. The Jacobian is then updated iteratively at each time step using (3). To avoid erratic motion near singular configurations where the Jacobian is ill-conditioned, its pseudoinverse is computed via the damped least-squares method, as $\mathbf{J}^\dagger = \mathbf{J}^T(\mathbf{J}\mathbf{J}^T + \lambda^2\mathbf{I})^{-1}\mathbf{J}^T$. By combining (2) with the Jacobian adaptation law (3), the tip position $\mathbf{p}(t)$ converges to the desired trajectory $\mathbf{p}_d(t)$ [4].

The overall control framework is illustrated in Fig. 2. The control input $\dot{\mathbf{F}}(t)$ in (2) is not directly applicable to the actuator. Therefore, it is first integrated as $\mathbf{F}(t) = \mathbf{F}(t-1) + dt \cdot \dot{\mathbf{F}}(t)$, where $\mathbf{F}(t)$ represents the desired tendon force to be achieved. The desired force is regulated using load cell feedback by commanding the linear actuators according to

$$\mathbf{v}(t) = k_f(\mathbf{F}(t) - \mathbf{F}_m(t)) \quad (4)$$

where $\mathbf{v}(t)$ is the velocity command to the linear motor actuators, $\mathbf{F}_m(t)$ is the measured tendon force, and k_f is a positive gain. By driving the actuators to minimize the force error, the measured tendon force $\mathbf{F}_m(t)$ converges to the desired force $\mathbf{F}(t)$, which in turn drives the tip position $\mathbf{p}(t)$ toward the desired trajectory $\mathbf{p}_d(t)$.

IV. EXPERIMENTAL RESULTS

The experiment is conducted on a real-scale continuum robot using the setup shown in Fig. 1. The initial Jacobian is determined from the observed tip displacement in response to applied tendon forces, as follows:

$$\hat{\mathbf{J}}(0) = \begin{bmatrix} -1.08 & 0.54 & 0.54 & -0.46 & 0.23 & 0.23 \\ 0.00 & -0.76 & 0.76 & 0.00 & -0.40 & 0.40 \\ 0.01 & 0.01 & 0.01 & 0.00 & 0.00 & 0.00 \end{bmatrix} 10^{-2}.$$

The controller gains are tuned empirically. The desired trajectory is a circular path with a constant p_z . To evaluate the robustness of the proposed controller, an external load is applied at the tip of the continuum robot in the direction opposite to the x-axis.

The experimental results in Fig. 3 show that the tip position components p_x , p_y , and p_z successfully track the desired

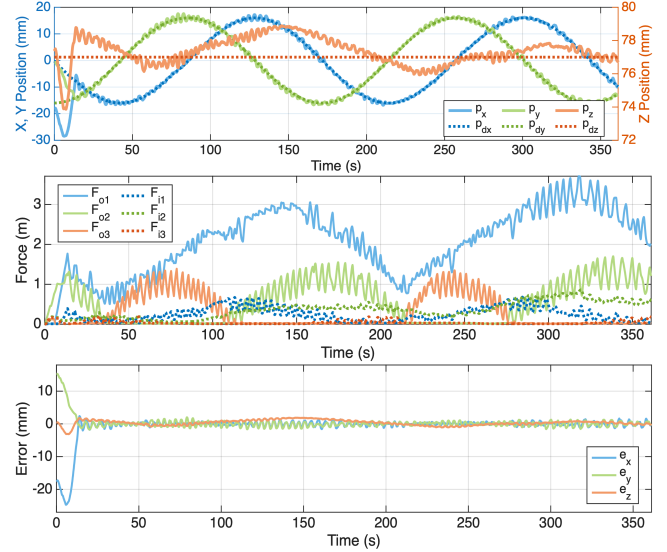


Fig. 3. Experimental results showing the comparison of measured and desired positions (top), input tendon forces (middle), and tracking error (bottom).

trajectory, with root mean square errors of [0.55, 0.66, 0.83] mm along the three axes. A large initial error is observed because of the difference between the initial position and the desired trajectory, as well as the discrepancy between the initial estimated Jacobian and the actual Jacobian. After approximately 12 s, the tracking error converges to near zero, although oscillatory behavior persists. This oscillation is mainly attributed to the numerical differentiation used to estimate velocity and acceleration and to the Euler integration applied to the force input, which also causes oscillations in the tendon force inputs.

V. CONCLUSION

This paper presented a Jacobian-based tracking control framework for a two-section, concentrically tendon-driven continuum robot. An online Jacobian estimation method based on input–output data was employed to address modeling uncertainties without requiring an explicit model. Experimental results on a real-scale system demonstrate effective tip tracking performance, even with external loads, highlighting the robustness and practical applicability of the proposed approach.

REFERENCES

- [1] I. A. Kuncara, Y. Ko, A. Widyotriatmo, and C.-S. Kim, “Dynamic modeling and validation of a notched hollow continuum robot using cosserat rod theory,” *IEEE/ASME Transactions on Mechatronics*, pp. 1–14, 2025.
- [2] B. Ozdemir, M. A. Khalid, M. Chauhan, P. Valdastrì, and J. H. Chandler, “Hybrid continuum robot designs and architectures for healthcare applications,” *Advanced Robotics Research*, p. e202500177, 2026.
- [3] Y. Zhai, J. Xu, H. Mo, C. Zhang, and D. Sun, “Model-based control of a continuum manipulator with online jacobian error compensation using kalman filtering,” *Cyborg and Bionic Systems*, vol. 6, p. 0339, 2025.
- [4] D. Chen, Y. Zhang, and S. Li, “Tracking control of robot manipulators with unknown models: A jacobian-matrix-adaption method,” *IEEE Transactions on Industrial Informatics*, vol. 14, no. 7, pp. 3044–3053, 2018.